

An Experimental Study on Industrial Concrete Pile Foundation in Soft Soil: Comparison of Monolithic and Pile with Welded Joints

Rustam Effendi

Civil Engineering Program, Faculty of Engineering, Lambung Mangkurat University, Indonesia
rustamff@ulm.ac.id

Ade Yuniati Pratiwi

Civil Engineering Program, Faculty of Engineering, Lambung Mangkurat University, Indonesia
ade.pratiwi@ulm.ac.id (corresponding author)

Nursiah Chairunnisa

Civil Engineering Program, Faculty of Engineering, Lambung Mangkurat University, Indonesia
nursiah.chairunnisa@ulm.ac.id

Nor Muhammad Alpindi

Civil Engineering Program, Faculty of Engineering, Lambung Mangkurat University, Indonesia
alpindi80@gmail.com

Ratni Nurwidayati

Civil Engineering Program, Faculty of Engineering, Lambung Mangkurat University, Indonesia
ratninurwidayati@ulm.ac.id

Wiku Adhiwicaksana Krasna

Civil Engineering Program, Faculty of Engineering, Lambung Mangkurat University, Indonesia
wakrasna@ulm.ac.id

Received: 30 August 2024 | Revised: 1 October 2024 | Accepted: 17 October 2024

Licensed under a CC-BY 4.0 license | Copyright (c) by the authors | DOI: <https://doi.org/10.48084/etasr.8855>

ABSTRACT

This study presents an experimental investigation into the industrial foundation piles. The research carried out employed both destructive and non-destructive testing methods to evaluate the concrete compressive strength and flexural strength capacity of the piles under monotonic loading. The Destructive Test (DT) involves a 28-day cylinder concrete compressive test, while the Non-Destructive Test (NDT) utilizes the Ultrasonic Pulse Velocity (UPV) and Rebound Hammer (RH) tests. The flexural strength test is conducted using a loading frame, and the results are compared to the GeoPIV-RG, which measures the displacement during the test. The experimental investigations provide insights into the behavior of pile joints when subjected to monotonic load in soft and loose soil. The results indicate a significant difference between the compressive strength obtained from the DT and NDT, with a ratio of 0.64-0.74. Furthermore, the failure occurred at the joints, rather than the welded area, with the ratio of the initial stiffness of the piles with joints to the monolithic pile being 0.15 for zig-zag welded and 0.30 for circular welded, and reaching an average value of 0.225. According to the GeoPIV-RG result, the displacement is similar to the flexural strength test result.

Keywords-monolithic; welded; industrial pile; destructive test; non-destructive test; compressive strength; flexural strength; initial stiffness ratio; Geopiv-rg; displacement

I. INTRODUCTION

Indonesia is situated in an earthquake-prone region. Structures in this area are subjected to substantial cyclical lateral forces as well as vertical loads emerging from the structure itself during a major seismic event. Furthermore, soft ground structures can amplify shaking, as the soft soil response is doubled from a distant earthquake epicenter. Pile foundations, a deep foundation type widely employed in construction, are utilized when the surface soil is unable to support the building or structure weight. The flexural strength performance of concrete pile foundations has been internationally investigated [1-5]. Based on geotechnical assessments, a pile foundation is necessary to support a heavily loaded building column. Several factors, including soil conditions, the superstructure's high inertia force, improper pile design, and inadequate pile jointing, can result in pile foundation damage during an earthquake. Despite their widespread use and technical maturity, typical prestressed concrete pipe piles have certain drawbacks, such as the potential for joint failure. Numerous studies have been conducted to examine the impact of seismic events on pile foundation behavior. For instance, the findings of the Loma Prieta and Northridge earthquakes revealed that significant damage had been caused to the pile foundation or substructure [6, 7-13].

Reinforced concrete piles are commonly utilized as foundations for land buildings requiring high-quality cement and seaside structures [14]. The installation of lengthy precast concrete piles can be problematic, possibly leading to certain issues, such as carrying costs, considerable pile weights, and cracking during handling. To address these challenges, shorter pile lengths are spliced together. Furthermore, precast concrete joint piles exceeding 12 meters are necessary in construction due to the growing number of floors and the extensive employment of pile foundations in soft soil conditions. Various connection methods can be applied to piles, including mechanical splices, welded splices, epoxy-bonded splices, grouted splices, and bolted splices, each presenting unique considerations [15-17]. Several factors influence the overall effectiveness of a given splice, such as the size range, field splicing time, approximate cost, accessibility, construction use, structural performance, and structural integrity [18]. It is worth mentioning that the splicing of pile foundations must meet the requirements for compressive, tensile, and moment forces, as well as those for lateral forces resulting from external loads and the weight of the superstructure, to prevent connection failures [16, 17, 19].

Previous studies have shown that reinforced concrete piles with inadequate splicing details, particularly at the pile-to-pile cap connection, can lead to poor performance of the pile foundation system [10]. Furthermore, many piles appear to have failed due to insufficient core concrete confinement and a lack of careful detailing in the splicing process. The effect of welded splices was investigated with a predetermined gap on concrete spun piles using Pile Integrity Testing (PIT) [15]. The ability of the entire welded splice to transmit stress wave velocity was demonstrated. Despite the development of a

reflecting wave at the splice, the reflecting wave at the pile toe can serve as an indicator of a well-executed welded splice.

Prior research has typically focused on the mechanical characteristics of precast piles, while splicing has received less attention. The pile material type, required splice strength, and project-specific requirements all influence the various existing pile splicing techniques [20]. Welded splices are widely used in Indonesia due to their cost-effectiveness and versatility. The key performance indicators for precast piles in deep foundation pits are their flexural and shear behaviors [21]. Furthermore, former research has outlined that the primary cause of pile failure is often their flexural behavior [22, 23]. This study aims to investigate concrete quality using DT and NDT, flexural capacity utilizing flexural strength tests, and the failure mechanism of two types of concrete pile foundations, namely monolithic piles without joint connections and welded piles. The experimental investigations provide insights into the behavior of the joint when subjected to monotonic loads, particularly in soft soil conditions.

II. MATERIALS AND METHODS

This study employed an experimental research design involving multiple components, like a survey to gather data on typical industrial foundation piles, manufacturing of the piles in a dedicated concrete pile factory, compressive strength testing of the concrete using both DT and NDT, flexural strength testing of the piles, and the subsequent data analysis.

A. Industrial Concrete Pile Specimen

Industrial concrete piles are manufactured based on the specifications of a foundation concrete pile in a factory setting. There are three types of specimens: monolithic, with zig-zag welding connection, and with circular welding connection. Each type consists of two specimens. The monolithic specimens have dimensions of $40 \times 40 \times 250$ cm, while the zig-zag and circular welding connection specimens have dimensions of $40 \times 40 \times 125$ cm. The zig-zag and circular welding connection specimens are characterized by male and female parts, as shown in Figure 1. These male and female parts are connected and welded using zig-zag and circular welding styles, as depicted in Figure 2, resulting in a total pile length of 2.5 m. Concrete compressive strength is 40 MPa. The piles utilized four seven-wire prestressed strands of Grade 270, with a diameter of 12.7 mm, as longitudinal reinforcement, and 6 mm steel bars with a yield strength of 240 MPa as circular transverse reinforcement. The specification of the piles is presented in Table I.

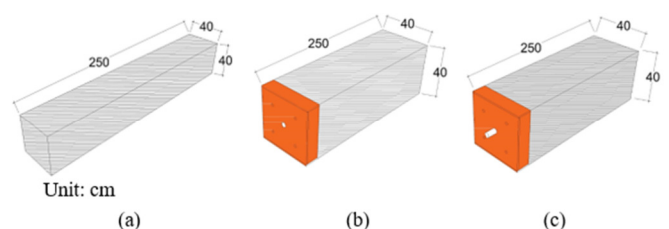


Fig. 1. Industrial concrete pile specimen: (a) Monolithic, (b) female, and (c) male.

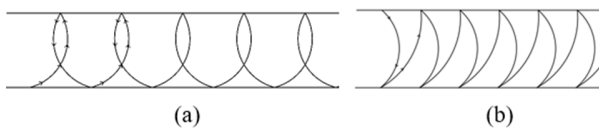


Fig. 2. Welding type: (a) Circular and (b) zig-zag.

TABLE I. SPECIFICATION OF PILES

Specification of pile	
Concrete Compressive Strngth (f'_c)	41.5 MPa
Yield strength of steel bar (f_y)	240 MPa
Ultimate strength of 7-wire strand (f_u)	1860 MPa
Cracking Moment	16.32 t.m
Ultimate Moment	7.55 t.m

B. Compressive Strength: DT and NDT

The compressive strength of concrete is evaluated through the adoption of two methods: the DT using 28-day cylinder concrete compressive testing and the NDT employing UPV and RH techniques. The UPV test, an NDT approach, estimates the hardness of concrete by measuring the velocity of UPV waves propagating through the material. This provides insights into the concrete's uniformity, quality, and the potential presence of voids or cracks, which is crucial for determining the effectiveness of crack repair. The UPV testing procedure involves identifying the object to be tested, calibrating the equipment, measuring the travel time, and calculating the wave propagation speed. The results are expressed as a propagation speed index, demonstrating the concrete's quality as a building material. The UPV testing was carried out in compliance with the codes for testing concrete in structures [24-27]. The non-destructive UPV test utilizes a receiving transducer to accurately detect the arrival of an earlier pulse component. An electro-acoustic transducer generates a robust longitudinal vibration pulse that propagates through the concrete, eliciting a complex stress wave system comprising longitudinal and shear waves. The transit time (T) of the pulse is precisely measured using an electronic timing circuit, and the wave propagation velocity (v) of longitudinal waves in the concrete can be confidently calculated based on its elasticity and density properties, as described by:

$$v = \sqrt{\frac{E(1-\mu)}{\rho(1+\mu)(1-2\mu)}} \quad (1)$$

The modulus of elasticity, denoted as E and a value of $4700\sqrt{f'_c}$, represent concrete resistance to deformation. The density, ρ , is obtained by calculating the ratio of the concrete's mass to its volume, having a value of 2200 kg/m^3 . The UPV, V , is determined by dividing concrete thickness by the travel time of the UPV. The Poisson's ratio, μ , typically ranges from 0.15 to 0.20 for normal concrete. Concrete quality is assessed based on the guidelines established in IS 516, while its uniformity is evaluated in accordance with SNI 03-6825-2002 [26-28]. In this study, the UPV test was performed following the indirect transmission method.

The RH test tool is employed to assess the consistency of concrete hardness, which is linked to its compressive strength. In accordance with ASTM C805, the device should be utilized

to acquire ten measurement points within each test area, maintaining a minimum spacing of 25 mm between each point. After the experienced impact, the concrete surface must be inspected, and if the impact compromises or damages the surface due to air voids, the reading should be invalidated, and an additional measurement point should be taken. Readings that deviate by more than six units from the average of the 10 measurement points should be disregarded, and the average value should be calculated based on the remaining valid data points [29]. If more than two measurement points differ by more than six units from the average value, the entire set of readings should be canceled, and the rebound number should be determined for ten new measurement points in the test area.

TABLE II. CONCRETE QUALITY BASED ON IS 516

Concrete quality	Pulse velocity (m/s)	Concrete Conditions
	>4500	Excellent
3500-4500	Good	
3000-3500	Medium	
<3000	Doubtful	

C. Flexural Strength Test

Pile foundation flexural strength testing is carried out using a loading frame, load cell, data logger, and hydraulic pump. Flexural strength testing is for/addresses to monolithic, zig-zag welded, and circular welded specimens. The setting for flexural strength testing is presented in Figure 3.

D. GeoPIV-RG

The GeoPIV-RG system employs a MATLAB-based image analysis module to provide sub-pixel measurement precision, making it well-suited for examining problems involving significant displacements and deformations. This technique is commonly deployed to quantify deformation in granular materials, such as soil or sand, through the application of Particle Image Velocimetry (PIV). PIV relies on image processing, whereby measurements are obtained by analyzing flow recordings. In this study, the GeoPIV-RG software was utilized to capture a series of images of the test material sample and then track the movement of particles between the images using an algorithmic approach. The material sample was marked with random dots, representing the granular particles, which were subsequently captured by the camera and processed applying the GeoPIV-RG software.

III. RESULTS AND DISCUSSION

A. Compressive Strength: DT and NDT Results

NDT testing is performed to assess concrete quality without compromising the sample's structure. The primary methods utilized were the RH and UPV tests. The test result data are presented in Tables III and IV. Based on the RH test results, the average concrete compressive strength is 60.27 MPa for all specimens with 80% reliability, while the average UPV compressive strength test result is 52.41 MPa. The average velocity is 3867.66 m/s, which, according to Table IV, exhibits that concrete quality is good, with uniformity ranging from fair to excellent.

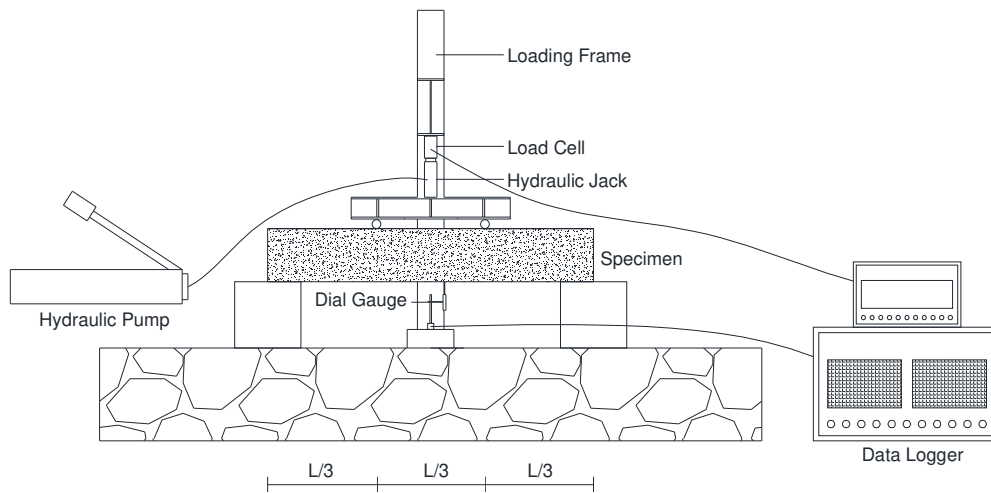


Fig. 3. Flexural strength test set up.

TABLE III. RH TEST RESULTS

No.	Average of RH	Estimation of Concrete Compressive Strength		Reliability %
		kg/cm ²	MPa	
1	48	581.75	57.05	80.00
2	50	631.86	61.97	80.00
3	50	624.70	61.26	80.00
4	49	606.80	59.51	80.00
5	50	631.86	61.97	80.00
6	49	610.39	59.86	80.00

TABLE IV. UT/LTRASONIC PULSE VELOCITY TEST RESULTS

No	Average Concrete Compressive Strength (MPa)	Concrete Quality		Uniformity of Concrete Quality	
		Average Velocity (m/s)	Description	Std. Dev. (%)	Description
1	49.80	3819.2	Good	31.22	Good
2	52.71	3874.2	Good	24.53	Very Good
3	52.41	3867.6	Good	44.39	Fair
4	49.46	3812.6	Good	9.42	Excellent
5	54.71	3908.7	Good	53.30	Fair
6	53.67	3891.8	Good	22.60	Very Good
7	54.13	3899.5	Good	35.19	Good

In contrast, the 28-day Cylinder Concrete Compressive Strength Test Results, shown in Table V, reveal an average compressive strength of 38.68 MPa, lower than the RH and UPV test results. These findings align with similar research endeavors suggesting that the discrepancy between DT and NDT tests may be influenced by concrete age and the presence of reinforcement, which can enhance the estimated concrete compressive strength [30-32].

TABLE V. 28-DAY CYLINDER CONCRETE COMPRESSIVE STRENGTH TEST RESULTS

28-days Sample	Weight (g)	Load (kN)	Concrete Compressive Strength (MPa)
1	11536	885	42.33
2	11720	755	35.44
3	11602	800	38.26

Figure 4 illustrates the ratio of concrete compressive strength derived from NDT methods compared to DT results. This ratio constitutes a crucial piece of information to obtain results similar to those attained from DT. It can be also inferred that the UPV test results are higher than the RH test results, and closely approximate the DT results. It is recommended that the ratio shown in Figure 4 be applied to multiply the compressive strength derived from the NDT methods.

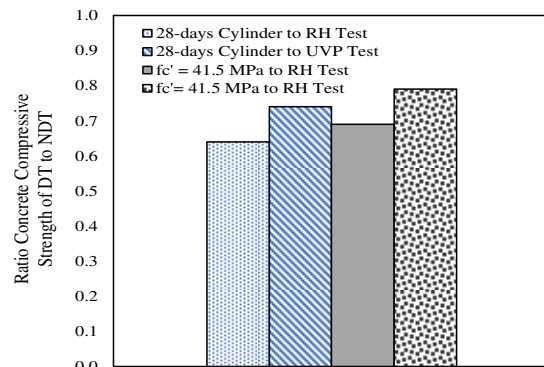


Fig. 4. Ratio of concrete compressive strength based on NDT to DT comparison.

B. Flexural Strength Test Results

The flexural strength test results portrayed in Table VI reveal that the monolithic pile type in the experiment withstood significantly higher loads compared to the piles with welded joints, or remained in the crack phase without reaching ultimate failure. In contrast, both the zig-zag and circular welded piles exhibited similar maximum force capacities, averaging 20.25 tons and 21.78 tons, respectively. The average maximum deformation for the zig-zag and circular welded piles was 18.785 mm and 20.51 mm, respectively. The flexural strength test evidenced in Figure 5 indicates that the failure mechanism of monolithic specimens may involve concrete and reinforcement failure or flexural failure, whereas the welded specimens experienced a separation of the concrete and pile joints, rather than failure in the welding area. As illustrated in

Figure 6, the relationship between load and deformation highlights the superior load capacity and initial stiffness of the monolithic piles compared to the welded piles. These findings underscore the potential challenges encountered when the pile is subjected to lateral loads and utilizes joints instead of a monolithic design, emphasizing the need for careful engineering to mitigate the risk of failure at the joints. In Figure 6, M denotes monolithic flexural capacity, ZZ the zig-zag welded, CR the circular welded, V_y the yield force, Δ_y the yield deformation, V_m the maximum force, Δ_m the maximum deformation, V_t is the ultimate force, and Δ_t is the ultimate deformation. During testing, the monolithic piles were unable to achieve/reach the yield stage until reaching the ultimate stage because of a limitation of the test setup. Only a first/an initial cracking is observed and based on these data, the initial stiffness of the monolithic pile will be derived and utilized.



Fig. 5. Flexural strength test: (a) monolithic pile and (b) welded pile.

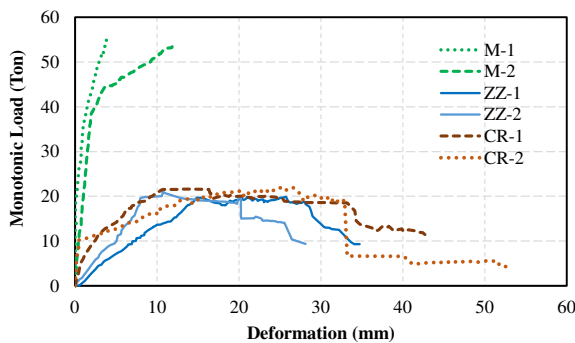


Fig. 6. Monolithic pile and welded pile flexural capacity under monotonic load.

TABLE VI. FLEXURAL STRENGTH TEST RESULTS

Pile type	V_y (t)	Δ_y (mm)	V_m (t)	Δ_m (mm)	V_t (t)	Δ_t (mm)	Phase
M-1	N/A	N/A	N/A	N/A	N/A	N/A	Crack
M-2	N/A	N/A	N/A	N/A	N/A	N/A	Crack
ZZ-1	18	9.5	19.26	26.65	18.74	28.06	Crack, Yield, Ultimate
ZZ-2	19.5	7.9	21.24	10.92	19.80	20.10	Crack, Yield, Ultimate
CR-1	20.3	6.4	21.66	14.34	18.5	31.51	Crack, Yield, Ultimate
CR-2	17.5	4.5	21.90	26.68	18.97	32.65	Crack, Yield, Ultimate

Table VII demonstrates the initial cracking and failure mechanisms of piles. Monolithic piles exhibit an initial cracking in the middle of the beam, consistent with the characteristic of beams exhibiting flexural failure. All welded specimens displayed analogous behavior, since the piles

separated precisely at the joints but not at the welded connections. These findings highlight the importance of focusing on the strength of the joints, as this can enhance the capacity of industrial piles subjected to lateral loads. In situations where the soil is classified as loose and soft, lateral loads can pose a significant challenge for piles, as they may have multiple joints to penetrate the hard soil. Consequently, the flexural strength test results were analyzed using idealized force-deformation relationships to gain insights into the stiffness characteristics, as displayed in Table VIII.

TABLE VII. FIRST CRACKING AND FAILURE MECHANISM

No	Specimens	Load in first cracking phase (t)	Description
1	M-1	45.61	First Crack in the middle of beam
2	M-2	40.02	First Crack in the middle of beam
3	ZZ-1	12.20	Separation of concrete and pile joints
4	ZZ-2	12.40	Separation of concrete and pile joints
5	CR-1	15.55	Separation of concrete and pile joints
6	CR-2	12.34	Separation of concrete and pile joints

In Table VIII, K_i refers to the initial stiffness, K_e to the effective stiffness, and αK_e to the post-yielding stiffness. K_i is approximated from the secant of the force and deformation before yielding, K_e is estimated at a base shear force that is 60% of the effective yield strength of the structure, and lastly regarding αK_e , it is the secant of the force and deformation after the yield stage. According to Table VIII, the zig-zag specimens exhibit positive αK_e , while the circular specimens display both positive and negative αK_e . The αK_e of the welded specimens varies, but the differences are not highly significant due to the similar failure mechanism.

TABLE VIII. STIFFNESS BASED ON IDEALIZED FORCE-DEFORMATION [33]

No	Specimens	K_i (t/mm)	K_e (t/mm)	αK_e (t/mm)
1	M-1	10.17	N/A	N/A
2	M-2	19.94	N/A <td N/A	
3	ZZ-1	2.33	1.89	0.04
4	ZZ-2	2.17	2.47	0.02
5	CR-1	3.75	3.17	-0.07
6	CR-2	5.32	3.89	0.05

Table IX provides recommendations for designing and calculating the capacity of piles subjected to soft soil conditions. Based on the information provided in Table IX, the coefficients for all-welded and monolithic piles can be used as general guidelines when designing the capacity of piles.

TABLE IX. AVERAGE INITIAL STIFFNESS RATIO OF WELDED PILE TO MONOLITHIC PILE

No.	Description	Ratio of K_i
1	$\frac{\bar{X}_{zig-zag\ welded}}{\bar{X}_{monolithic}}$	0.15
2	$\frac{\bar{X}_{circular\ welded}}{\bar{X}_{monolithic}}$	0.30
3	$\frac{\bar{X}_{all\ welded}}{\bar{X}_{monolithic}}$	0.225

C. GeoPIV-RG

The GeoPIV-RG software is programmed to accurately calculate the displacement of regularly spaced grid subsets. Consequently, it requires an interpolation method to determine the displacement of user-specified subset locations from the regularly gridded output. Figures 7 and 8 illustrate the particle image processing of the welded piles, ZZ-2 and CR-2.

The analysis demonstrates that the GeoPIV-RG successfully captured the position and the contours of displacement based on the sequence of images captured by the camera until the specimen's failure. According to the GeoPIV-RG results, the displacement of ZZ-2 was approximately 26 mm, while for CR-2, it was around 30 mm. This result is consistent with the flexural strength test findings presented in Table VI.

IV. CONCLUSION

Numerous studies have examined the flexural capacity of diverse structures, but less attention has been paid to the flexural behavior and failure mechanisms of concrete

foundation piles, particularly to the comparative analyses of monolithic piles and those featuring welded joints. These experimental investigations offer insights into the response of such joints when subjected to monotonic loading in soft, loose soil conditions. Furthermore, limited research has explored the concrete quality of factory-produced piles, especially by comparing the Destructive Test (DT) and Non-Destructive Test (NDT) methods. The present study aims to address these gaps and provide comprehensive information on these topics. The novel contributions of this research include the provision of ratios derived from comparing DT and NDT techniques, the ratio of initial stiffness between welded-joint and monolithic piles, and the potential utilization of GeoPIV-RG to measure displacement during the flexural testing of piles.

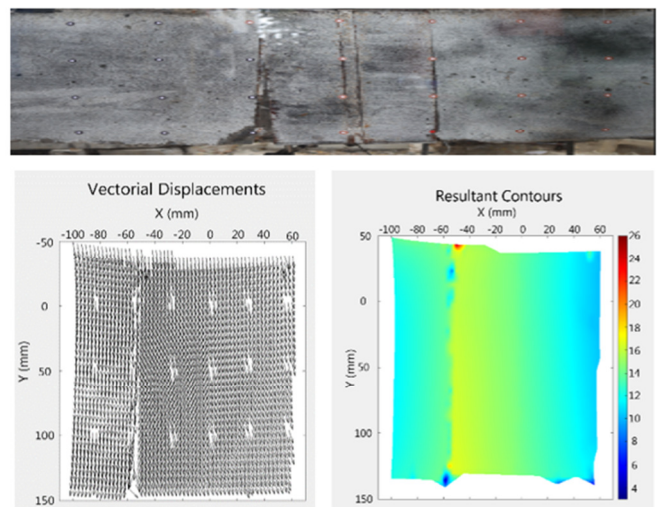


Fig. 7. Particle image processing of ZZ-2 using GeoPIV-RG.

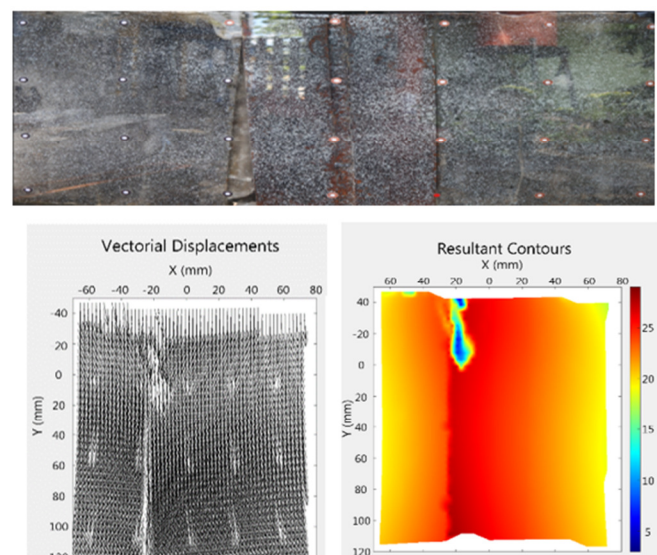


Fig. 8. Particle image processing of CR-2 using GeoPIV-RG.

The present study examined industrial piles deploying both the DT and NDT compressive strength testing methods. The

results indicate that the NDT approach tends to yield higher values compared to the DT method. Based on the DT to NDT finding ratio, which ranged from 0.64 to 0.74, it is recommended that a modification factor be applied to the concrete compressive strength measurements.

The flexural strength tests on the piles revealed that the failure occurred at the joints rather than the welded areas. The ratio of the initial stiffness of the piles with joints to the monolithic piles was 0.15 for zig-zag welded and 0.30 for circular welded, with an average value of 0.225. It is recommended that this initial stiffness ratio be incorporated in the capacity calculation of piles subjected to lateral loads in soft and loose soil with pile joints. Furthermore, the use of GoePIV-RG in the flexural strength test or other structural testing is suggested for the displacement to be obtained, as it provides results similar to those of the flexural strength test.

ACKNOWLEDGEMENT

The authors would like to thank Lambung Mangkurat University through Fundamental Research Grant Program by LPPM ULM under contract number 1374.3/UN8.2/PG/2024.

REFERENCES

- [1] H. Kishida, "Damage to Reinforced Concrete Buildings in Niigata City with Special Reference to Foundation Engineering," *Soils and Foundations*, vol. 6, no. 1, pp. 71–88, Jan. 1966, <https://doi.org/10.3208/sandf1960.6.71>.
- [2] P. H. Joen and R. Park, "Flexural strength and ductility analysis of spirally reinforced prestressed concrete piles," *PCI Journal*, vol. 35, no. 4, pp. 64–83, 1990.
- [3] H. Wang, G. Gan, K. Zeng, K. Chen, and X. Yu, "Study on Flexural Performance of Prestressed Concrete Steel Strand Square Piles with Reinforcement," *Buildings*, vol. 12, no. 11, Nov. 2022, Art. no. 1801, <https://doi.org/10.3390/buildings12111801>.
- [4] Y. Xu, Z. Chen, J. Fan, Z. Li, K. Zhang, and X. Tu, "Study on the Flexural Performance of Prestressed Concrete Solid Square Piles and Resilient Clamping Connections," *KSCCE Journal of Civil Engineering*, vol. 27, no. 1, pp. 285–298, Jan. 2023, <https://doi.org/10.1007/s12205-022-0148-8>.
- [5] B. Wang, L. Qi, and Y. Yang, "Experimental Study on Bending Resistance of New Type Joint of Prestressed Concrete Pipe Pile," *Symmetry*, vol. 14, no. 9, Sep. 2022, Art. no. 1920, <https://doi.org/10.3390/sym14091920>.
- [6] H. Mizuno, "Pile Damage During Hyougoken-Nanbu Earthquake in Japan (1923-1983)," in *Dynamic Response of Pile Foundations? Experiment, Analysis and Observation*, Atlantic City, New Jersey, United States, Apr. 1987, vol. 11, p. 186.
- [7] A. Budek and G. Benzoni, "Obtaining ductile performance from precast, prestressed concrete piles," *PCI Journal*, vol. 54, no. 3, pp. 64–80, 2009, <https://doi.org/10.15554/pcij.06012009.64.80>.
- [8] Yulius, W. A. Prakoso, M. Orientilize, and B. O. B. Sentosa, "Numerical Study Of Spun Pile To Pile Cap Connections In Soft Soil," *Journal of Physics: Conference Series*, vol. 1858, no. 1, Dec. 2021, Art. no. 012087, <https://doi.org/10.1088/1742-6596/1858/1/012087>.
- [9] P. H. Ziehl *et al.*, "Behavior of Pile to Bent Cap Connections Subjected to Seismic Forces," University of South Carolina, South Carolina, USA, FHWA-SC-12-03, Jun. 2012.
- [10] M. Teguh, C. Duffield, P. Mendis, and G. L. Hutchinson, "Seismic performance of pile-to-pile cap connections: An investigation of design issues," *Electronic Journal of Structural Engineering*, vol. 6, pp. 8–18, Jan. 2006, <https://doi.org/10.56748/ejse.654>.
- [11] T. C. Wang, Z. J. Yang, H. L. Zhao, and W. J. Wang, "Seismic performance of prestressed high strength concrete piles," *Materials Research Innovations*, vol. 18, no. sup2, pp. S2-515-S2-521, May 2014, <https://doi.org/10.1179/1432891714Z.000000000488>.
- [12] Z. Guo, W. He, X. Bai, and Y. F. Chen, "Seismic Performance of Pile-Cap Connections of Prestressed High-Strength Concrete Pile with Different Details," *Structural Engineering International*, vol. 27, no. 4, pp. 546–557, Nov. 2017, <https://doi.org/10.2749/222137917X14881937845963>.
- [13] Z. Yang, G. Li, and B. Nan, "Study on Seismic Performance of Improved High-Strength Concrete Pipe-Pile Cap Connection," *Advances in Materials Science and Engineering*, vol. 2020, no. 1, 2020, Art. no. 4326208, <https://doi.org/10.1155/2020/4326208>.
- [14] M. Tomlinson and J. Woodward, *Pile Design and Construction Practice*, 5th ed. London, UK: CRC Press, 2007.
- [15] G. S. Budi and L. S. Tanaya, "The Effect of Welded Splice with Predetermined Gap of Concrete Spun Pile on The Response of Low Strain Integrity Test," *Civil Engineering Dimension*, vol. 24, no. 2, pp. 109–114, Dec. 2022, <https://doi.org/10.9744/ced.24.2.109-114>.
- [16] A. Omarov *et al.*, "Bearing Capacity of Precast Concrete Joint Micropile Foundations in Embedded Layers: Predictions from Dynamic and Static Load Tests according to ASTM Standards," *Infrastructures*, vol. 9, no. 7, Jul. 2024, Art. no. 104, <https://doi.org/10.3390/infrastructures9070104>.
- [17] K. T. Chiarli and A. J. Susilo, "Analisis Kekuatan Sambungan Tiang Pancang Beton Terhadap Gaya Tarik, Lateral, Dan Momen Pada Tanah Kohesif," *JMTS: Jurnal Mitra Teknik Sipil*, pp. 607–614, Sep. 2021, <https://doi.org/10.24912/jmts.v0i0.10545>.
- [18] R. N. Bruce and D. C. Hebert, "Splicing of Precast Prestressed Concrete - I. Review and Performance of Splices," *PCI Journal*, vol. 19, no. 5, pp. 70–97, Sep. 1974, <https://doi.org/10.15554/pcij.09011974.70.97>.
- [19] J. E. Bowles, *Foundation Analysis and Design*, 5th edition. New York, USA: McGraw-Hill, 1995.
- [20] E. Blair, "Pile Splicing: Fundamentals, Methods, Equipment, and Quality Control," *Pilebuck, The International Deep Foundation and Marine Construction Magazine*, vol. 4, no. 1, 2024.
- [21] J. Liu, C. Shi, C. Cao, M. Lei, and Z. Wang, "Improved analytical method for pile response due to foundation pit excavation," *Computers and Geotechnics*, vol. 123, Jul. 2020, Art. no. 103609, <https://doi.org/10.1016/j.compgeo.2020.103609>.
- [22] M. Akiyama, S. Abe, N. Aoki, and M. Suzuki, "Flexural test of precast high-strength reinforced concrete pile prestressed with unbonded bars arranged at the center of the cross-section," *Engineering Structures*, vol. 34, pp. 259–270, Jan. 2012, <https://doi.org/10.1016/j.engstruct.2011.09.007>.
- [23] Z. Xizhi, Z. Shaohua, X. Shengbo, and N. Sixin, "Study of seismic behavior of PHC piles with partial normal-strength deformed bars," *Earthquake Engineering and Engineering Vibration*, vol. 19, no. 2, pp. 307–320, Apr. 2020, <https://doi.org/10.1007/s11803-020-0563-0>.
- [24] "Testing Concrete—Recommendations for Measurement of Velocity of Ultrasonic Pulses in Concrete." British Standards Institution, 1986.
- [25] "FEMA 356/Standard Test Method for Ultrasonic Pulse Velocity Through Concrete." Federal Emergency Management Agency, Reston, Virginia, 2022, <https://doi.org/10.1520/C0597-22>.
- [26] "Method of Tests for Strength of Concrete." Bureau of Indian Standards, 1959.
- [27] "Method of Non-destructive testing of concrete, Part 1: Ultrasonic pulse velocity." Bureau of Indian Standards, 1992.
- [28] "Metode Pengujian Kekuatan Tekan Mortar Semen Portland untuk Pekerjaan Sipil." Badan Standardisasi Nasional, Jakarta, Indonesia, 2002.
- [29] "Standard Test Method for Rebound Number of Hardened Concrete." American Society for Testing and Materials, West Conshohocken, PA, USA, 2019.
- [30] S. Katare *et al.*, "Comparative Study of Destructive Method and Non-destructive with Ultra-Sonic Pulse Velocity Method," *E3S Web of Conferences*, vol. 552, 2024, Art. no. 01110, <https://doi.org/10.1051/e3sconf/202455201110>.

- [31] J. Malek and M. Kaouther, "Destructive and Non-destructive Testing of Concrete Structures," *Jordan Journal of Civil Engineering*, vol. 8, no. 4, 2014.
- [32] R. F. Feldman, "Non-Destructive Testing of Concrete," *National Research Council Canada*, May 1977, <https://doi.org/10.4224/40000715>.
- [33] "Prestandard and Commentary for The Seismic Rehabilitation of Buildings." Federal Emergency Management Agency, Nov. 2000.